Chapter 16

Effect of Nano-TiN on Mechanical Behavior of Si_3N_4 Based Nanocomposites by Spark Plasma Sintering (SPS)

Jow-Lay Huang and Pramoda K. Nayak

Additional information is available at the end of the chapter

http://dx.doi.org/10.5772/50547

1. Introduction

Ceramic nanocomposites are often defined as a ceramic matrix reinforced with submicron/nano sized particles of a secondary phase. The advantages of these nanocomposites include: improved mechanical properties, surface properties, high thermal stability and superior thermal conductivity. It is very fascinating/interesting for the researchers to synthesize these composites as the incorporation of few percent nanosized particles changes the materials property substantially. Niihara et al.,[35], [36] have reported that the mechanical properties of ceramics can be improved significantly by dispersing nanometer-sized ceramic particles into ceramic matrix grains or grain boundaries. According to their observation, 5 vol% of silicon carbide nanoparticles into alumina matrix increases the room temperature strength from 350 MPa to approximately 1 GPa. Other strength improvements through similar approaches have been observed in alumina-silicon nitride, magnesia-silicon carbide, and silicon nitride-silicon carbide composite systems.

Apart from the basic mechanical properties such as such as micro hardness, facture strength, and facture toughness [9; 23; 44], nanocomposites also exhibit electro conductive, wear resistance, creep resistance and high temperature performance [10; 24; 37; 38, 39] However, the degree of improvement in these properties is dependent on the type of composite system involved.

1.1. Novel Synthesis of Ceramic nanocomposite

Chemical Vapor Deposition (CVD) is a very preferable method to disperse the nano-sized second phases into the matrix grains or at the grain boundaries [33]. However, the CVD process is not applicable to fabricate the large and complex shaped component for the mass produc-

tion and also it is very expensive. Processing route is another technique to prepare ceramic nanocomposites. Following the initial work of [34], several research groups have tried to synthesize the nanocomposites using different processing route such as conventional powder processing [6; 8], hot press sintering [25; 47] sol-gel processing [30; 50] and polymer processing [5; 16]. The ceramic nanocomposites can be synthesized using microwave plasma [48; 49]. The main advantage of this technique is that the reaction product does not form hard agglomerates because of the specific conditions during synthesis.

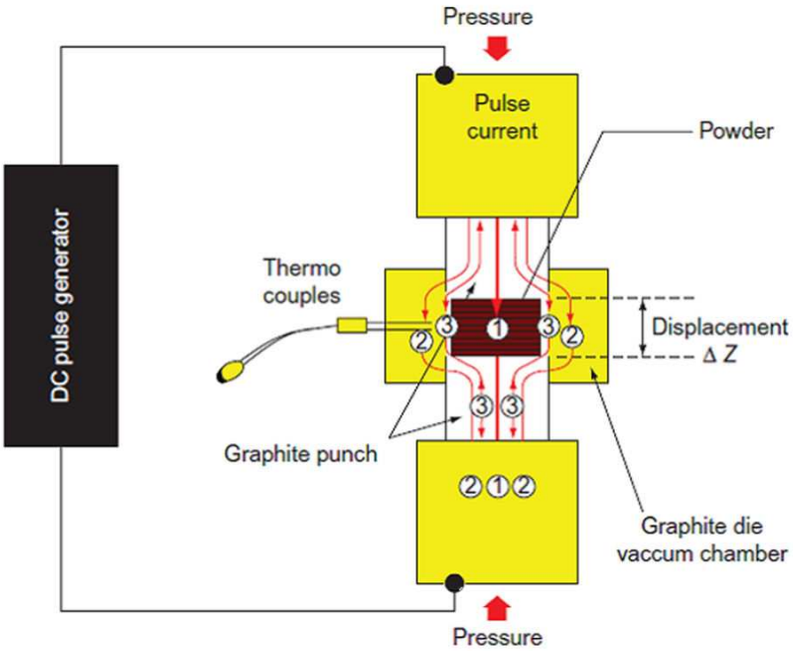

Figure 1. Schematics of Spark Plasma Synthesis (SPS) process

Recently developed Spark plasma sintering (SPS) is a novel sintering technique that uses the idea of pressure driven powder consolidation under pulsed direct electric current passing through a sample compressed in a graphite matrix. It is also known as the field assisted sintering technique or pulse electric current sintering. This newly developed sintering technique is regarded as an energy-saving technology due to the short process time and fewer processing steps. This technique was first described by Raichenko, 1987 and the key characteristics of this SPS are given as follows:

i. The generation of local electric discharge plasma and its effect on the material.

ii. The combined effect of external fields, such as a force field and electric field, on the densification and phase formation in a particulate system.

iii. The influence of electric current in the near surface layers of conductors and semiconductors (the so-called ''skin-effect'').

iv. The rapid and nonuniform heating/cooling throughout the sample, causing large temperature gradients.

http://dx.doi.org/10.5772/50547

The schematic of SPS process is shown in Fig.1 [41].

1.2. Advantages of SPS over other synthesis method

The most impressive advantage of SPS is its applicability to sinter materials of various types of chemical bonding and electric conductivity. Novel materials have been prepared from powders of ceramic dielectrics, conductors, semiconductors, amorphous alloys, and, sometimes, polymers. The traditional driving force involved in commonly used consolidation techniques such as solid state sintering and hot press sintering are: surface tension, external pressure, chemical potential due to the gradient of surface curvature, concentration gradient in multicomponent system etc. In SPS technique, the additional driving forces include electromechanical stress, high local temperature gradients creating thermal stresses intensifying thermal diffusion, and dislocation creep. These additional driving forces are responsible for much faster transport mechanism, that accelerates rapid sintering, which is observed in SPS.

1.3. TiN/Si_3N_4 Ceramic Nanocomposites

Si_3N_4 ceramics are regarded as one of the important high temperature structural materials. These ceramics have attracted much attention due to their good mechanical and chemical properties and due to their reliability at room and elevated temperatures [14; 19]. High strength and high-toughness Si_3N_4 matrix composites such as whisker-reinforced of particulate-reinforced ceramics, have been developed to improve the mechanical reliability of Si_3N_4 ceramics [2; 13]. However, these composites are extremely hard and machining using conventionals tools is difficult, which limits the widespread application of these materials in many fields. If, sintered Si_3N_4 bodies can be made electro conductive, electrical discharge machining (EDM) technique can be applied to manufacture complex components [32]. It has been reported that introduction of electro conductive second phase can improve the mechanical properties and electroconductivity of Si_3N_4 ceramics [14; 18; 43].

TiN exhibits a number of desirable properties, including high hardness, good chemical durability, high electrical conductivity and is a popular second phase additive due to its good compatibility with Si_3N_4. It often incorporated into the β-Si_3N_4 matrix as cutting-tool materials [4; 14; 17; 28]. There are two advantages to the Si_3N_4 based composites. First of all, the good physical properties of TiN, such as high melting point, hardness, strength and chemical stability, as well as its good erosion and corrosion resistance, enable it to be an excellent toughening material [7; 28; 51]. Secondly, the electrical resistance of Si_3N_4 can be substantially decreased, which consequently makes electric-discharge machining possible [17; 21].

2. Spark Plasma Sintering of TiN/Si_3N_4 nanocomposite

As described in the previous section, SPS is a newly developed sintering technique and it is beneficial to consolidate Si_3N_4 based nanocomposites in a short time. Some researchers have already reported that TiN/Si_3N_4 based nanocomposites with excellent mechanical properties and conductivity can be processed through a chemical route and sintered by SPS [1; 22].

However, due to the complexity of these processing techniques, they are not suitable for large scale production. The planetary milling process has been introduced in their study. Moreover, the details of microstructural development of Si_3N_4 and TiN have not described, especially in the presence of a pulse direct current through the sintering compact during a sintering cycle.

In the present study, we have prepared TiN/Si_3N_4 nanocomposite using SPS from Si_3N_4 and TiN nano powders. The Si_3N_4 and TiN nano powders were applied because they are sensitive to the microstructural changes during the sintering process. The relationship between microstructure and performance, like mechanical properties and electrical conductivity, of these TiN/Si_3N_4 nanocomposites are discussed. Finally, the effect of nano-TiN on the mechanical behavior of Si_3N_4 based nanocomposite has been investigated in sufficient details.

2.1 Experimental Details

2.1.1. Preparation of TiN/Si_3N_4 nanocomposite powder

Commercially available Si_3N_4 nano powder (SM131, Fraunhofer-Institut fur Keramische Technologien and Sinterwerkstoffe, Dresden, Germany) doped with sintering additives of 6 wt% Y_2O_3 and 8 wt% Al_2O_3 was taken as raw material for the matrix phase. It contains 90 wt% β-phase and 10 wt% α-phase, with a manufacturer-determined average particle size of 70nm by the Rietveld method. Nanosized TiN with size of ~30nm (Hefei Kiln Nanometer Technology Development, Hefei, China) was used as secondary phase and it was mixed with Si_3N_4 nano powders. The composition was chosen to yield a TiN content of 5, 10, 15, 20, and 30 wt % in the final product. The specimen designations and corresponding TiN/Si_3N_4 ratios in volume percentage (vol.%) for each composite are shown in Table 1. The mixing powders were ultrasonically dispersed in ethanol for 15 min, and then mixed by planetary milling at a rotation speed of 300rpm for 6 h using a 375 ml nylon bottle with Si_3N_4 balls. The powder mixture was dried in a rotary evaporator, iso-statically cold-pressed into round ingots at a pressure of 200 MPa, crushed and then passed through a #200 sieve for granulation.

TiN/Si_3N_4 content ratio (wt%)	Designation	TiN/Si_3N_4 content ratio (vol%)
5	5TN	3.31
10	10TN	6.75
15	15TN	10.06
20	20TN	14.00
30	30TN	21.81

Table 1. Specimen designation of composites for different TiN content.

http://dx.doi.org/10.5772/50547

2.1.2. Preparation of sintered bodies by SPS

The granulated powders were loaded into a graphite mold with a length of 50 mm and inner and outer diameters of 20 and 50 mm, respectively. A graphite sheet was inserted into the small gap between the punches and mold to improve the temperature uniformity effectively. The graphite mold was also covered with carbon heat insulation to avoid heat dissipation from the external surface of the die. After the chamber was evacuated to a pressure of 10 Pa, the sample was heated to 1600°C under a uniaxial pressure of 30 MPa by SPS (Dr. Sinter 1050, Sumitomo Coal Mining, Kawasaki, Japan). All the SPS measurements were carried out with a heating rate of 200°C/min and holding time of 3 min. A 12 ms-on and 2 ms-off pulse sequence was used. The heating process was controlled using a monochromatic optical pyrometer that was focused on the surface of the graphite mold.

2.1.3. Characterization of sintered bodies

The effective densities of the sintered composites were measured by the Archimedes principle. Phase identification was performed by an X-ray diffractometer (XRD; Model D-MAX/IIB, Rigaku, Tokyo, Japan). Cell dimensions were determined from XRD peak data using UNITCELL with a Si standard. A semiconductor parameter analyzer (HEWLETT PACKARD 4140B, USA) was used to determine the electrical resistivity of the samples. The upper surfaces of the sintered samples were polished down to 1μm. Hardness was measured with a Vickers hardness tester (AKASHI AVK-A, Japan) and by applying a micro-hardness indent at 196N for 15 s. Fracture toughness was measured by the Vickers surface indentation technique [12]. The polished and plasma etched surfaces were used for microstructural characterization by field emission scanning electron microscope (FESEM, XL-40FEG, Philips, The Netherlands). A thin specimen was prepared with a focused ion beam system (FIB, SEIKO, SMI3050, Japan). Transmission electron microscopy (FEGTEM, Tecnai G2 F20, Philips, Eindhoven, Netherlands) was used to characterize the TiN grain of the sintered sample.

2.2. Results and Discussion

2.2.1. Phase Identification of nanocomposite powders by XRD

Fig.2 shows the typical X-ray diffraction patterns of sintered TiN/Si_3N_4 composites with varying TiN content. These composites consist of the β-Si_3N_4 phase as a major phase along with coexistence with secondary TiN phase. The intensity of TiN peaks continues to increase with increasing TiN content. The value of the lattice constant for TiN is 4.25Å, approaching that of pure TiN. On the other hand, the values for a_0 and c_0 for the β-Si_3N_4 phase are 7.61 and 2.91Å, respectively, which are somewhat deviated from those for pure β-Si_3N_4 (+0.01Å). This result suggests that a tiny amount of Si–N may be replaced by Al–O in the particle dissolution and coarsening stages of liquid phase sintering and form the β-SiAlON phase [45].

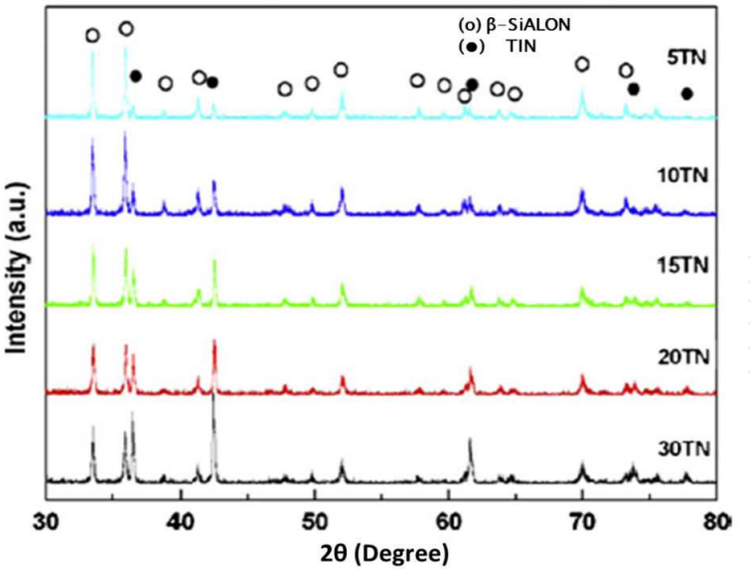

Figure 2. X-ray diffraction patterns of composites with different TiN content.

2.2.2. Densification Behavior

The apparent density of samples containing up to 30 wt% TiN is presented in Fig.3. The apparent density is found to increase with the increase of TiN content. The increase in density is as predicted, because the theoretical density of TiN (5.39 g/cm^3) is substantially greater than that of monolithic Si_3N_4 (3.19 g/cm^3) (Lide, 2002). No obvious pores are also observed on the polished surfaces of the samples (Fig.4), which suggest the TiN/Si_3N_4 composites are near full densification.

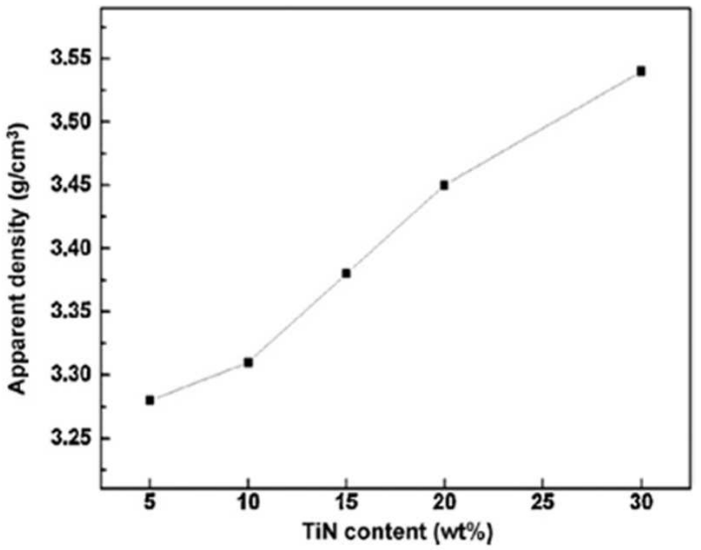

Figure 3. Variation of apparent density of the composites with TiN content.

http://dx.doi.org/10.5772/50547

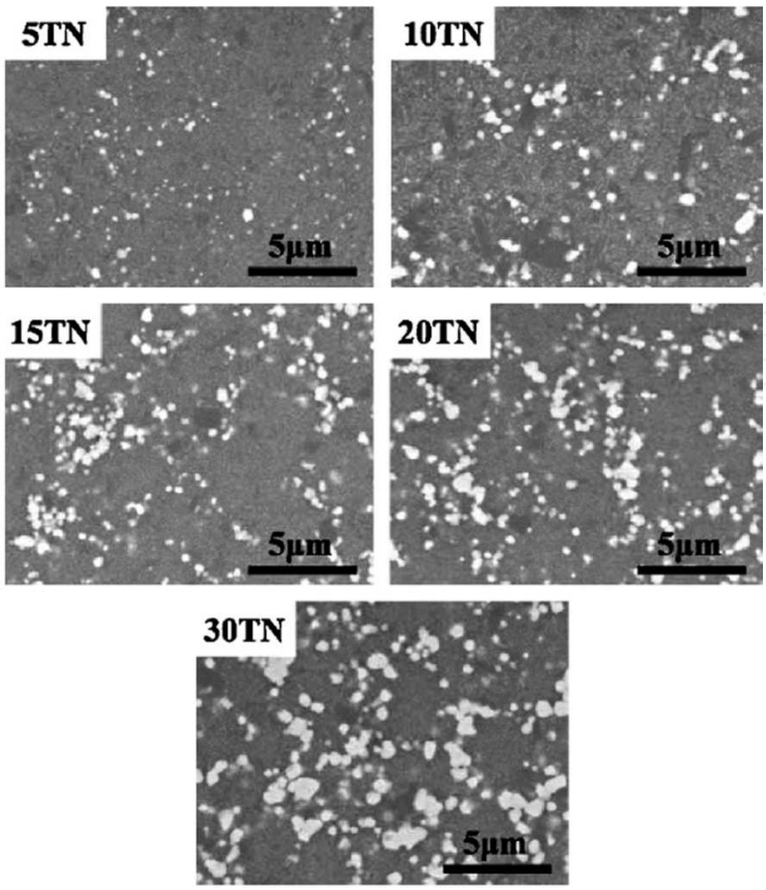

Figure 4. Backscattered SEM images of polished TiN/Si_3N_4 composites with varying TiN content. The brighter phase is TiN phase and the darker phase is β-SiAlON matrix.

2.2.3. Microstructure Observation of Nanocomposites

The backscattered electron images in SEM of the polished surface of composites with varying TiN content are shown in Fig. 4. As stated earlier, the samples were sintered at 1600°C for 3min with a heating rate of 200°C/min in a vacuum. The lighter and heavier atoms in the backscattered images show up as the gray and white regions corresponding to the β-SiAlON matrix (including glassy phase) and TiN particles. Therefore, the TiN particles are distributed homogeneously in the β-SiAlON matrix. However, most of the TiN appear as submicrosized grains, which are much larger than the size of the starting nano powders.

The typical bright field and dark field images of the TiN grain for the as-sintered composite containing 10 wt% TiN content are shown in Fig. 5(a) and (b), respectively. Fig. 5(c) presents the [0 1 1] selected area diffraction pattern (SAD) for the submicrosized TiN grain, and it shows the existence of a twin structure. The results suggest that grain growth and coalescence of TiN occurs in the composite during the spark plasma sintering process in a short time.

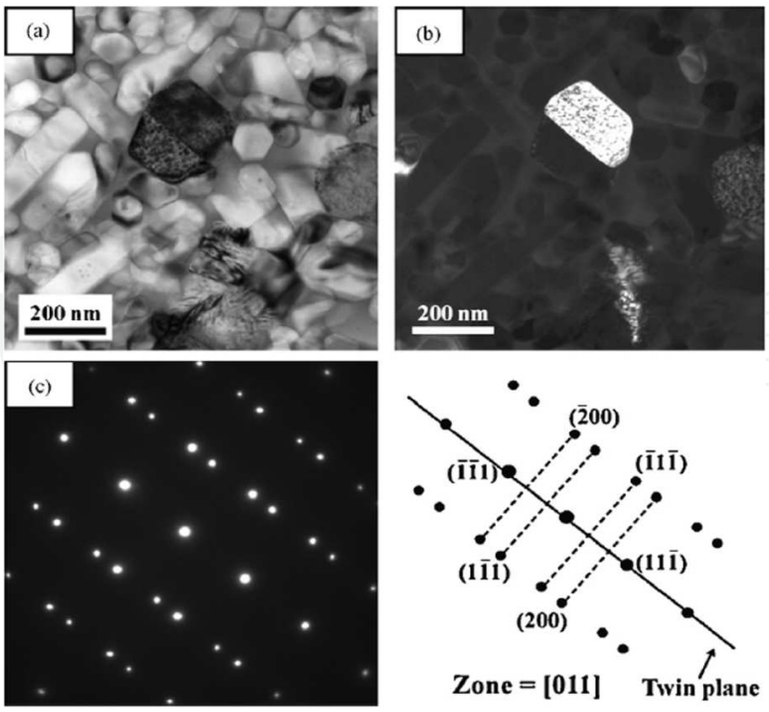

Figure 5. a) Bright field and (b) dark field micrographs, and (c) [0 1 1] selected area diffraction patterns of TiN in spark plasma sintered TiN/Si_3N_4 composite containing 10 wt% TiN.

The typical micrographs of β-SiAlON grains with different TiN content are presented in Fig. 6. In general, the TiN in TiN/Si_3N_4 based composite inhibits grain boundary diffusion and reduces the grain size of the Si_3N_4 matrix [20]. However, for the special case of 10TN among all these composites, the large, elongated grains can be obtained. The conductive phase of TiN might play an important role in the microstructural development of TiN/Si_3N_4 based composites. The electrical resistivity of TiN (3.34×10−7Ω.m) [14] is in the range of metallic materials. Although a tiny current appears as measured by a semiconductor parameter analyzer, it is reasonable that a large current might be induced in the presence of pulsed electrical field during sintering. A leakage current might go through the sintering compact during a heating process, and a similar phenomena is also proposed in ferroelectric ceramics [30; 45], and TiCxOyNz/Si_3N_4 based nanocomposites [31]. Therefore, it is expected that a direct current might hop across conductive TiN grains embedded in the insulating β-SiAlON matrix when applying a pulsecurrent. A temporary high temperature might occur in the specimen, and consequently accelerate the grain coarsening behavior of β-SiAlON during a sintering cycle.

Except for the case of the 10TN composite, most of the β-SiAlON grains for the composites have an equiaxial shape with a grain size of less than 200nm (as shown in Fig. 6), whereas a tiny amount of elongated grains with a grain width of 100nm were observed. For the composite of 5 TN, the percolation concentration is too low (i.e. the interparticle distance of TiN is large) to allow a pulse current to pass through the sintering body [52]. For the samples of 15 TN, 20 TN, and 30 TN, the TiN phase significantly inhibits the grain growth of the β-SiA-

http://dx.doi.org/10.5772/50547

lON matrix, even though it is possible for a pulse current to pass through the samples during sintering.

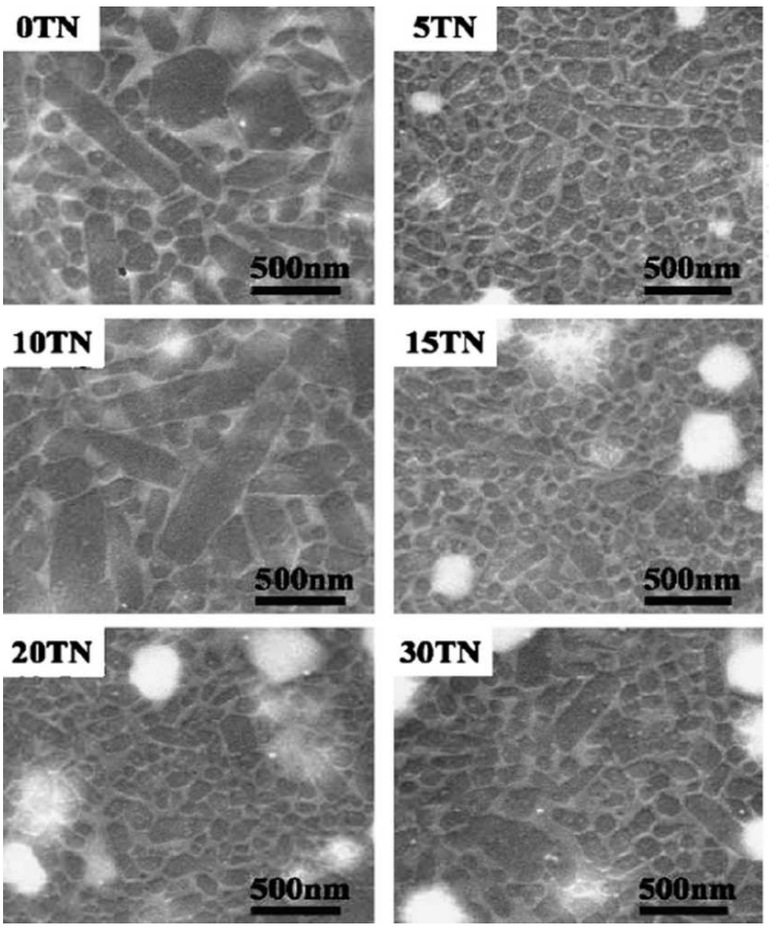

Figure 6. SEM micrographs showing the etching surface of TiN/Si_3N_4 composites with varying TiN content.

2.2.4. Electrical Properties

The change in electrical resistance for the above composites with varying TiN content is shown in Fig. 7. The electrical resistance substantially decreases from 2.43×10^{10}(5 TN) to 1.93×10^{8}(20 TN) (Ω.m) with the increase in TiN content, whereas it suddenly increases to a value of 4.19×10^{10} (Ω.m) for composite 30 TN. It has been reported that if the fraction of conductive TiN phase in the composite is under the degree of percolation threshold, the insulating property of the composites is maintained as the electrical resistance of non-conductive Si_3N_4 matrix [52]. This suggests the TiN phase does not form a connective network. As it is evidenced from Fig. 4, the submicrosized TiN grains are nearly isolated from each other. Moreover, the change of electrical resistance possibly depends on the grain size of the conductive phase [11]. Compared with the special cases for 20TN and 30 TN, the larger particle size of TiN for 30TN increases the interparticle distance, leading to a higher magnitude of electrical resistance over composite 20 TN.

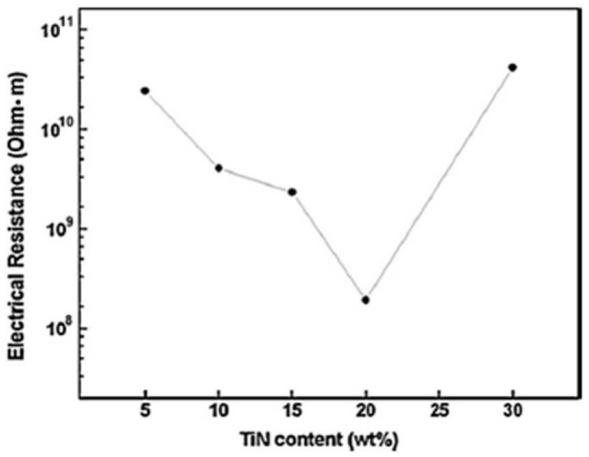

Figure 7. Change of electrical resistance of TiN/Si_3N_4 composites with varying TiN Content.

2.2.5. Mechanical Properties

The mechanical performance of the above nanocomposites has been studied from hardness and toughness measurements. Indentation hardness is a measure of resistance of a sample to permanent plastic deformation due to a constant compression load from a sharp object. This test works on the basic premise of measuring the critical dimensions of an indentation left by a specifically dimensioned and loaded indenter. Vickers hardness is a common indentation hardness scale, which was developed by Smith & Sandland [42]. Vickers test is often easier to use than other hardness tests since the required calculations are independent of the size of the indenter, and the indenter can be used for all materials irrespective of hardness. The influence of the TiN content of TiN/Si_3N_4 based nanocomposites on the Vickers hardness is shown in Fig. 8. The hardness value for these composites decreases with an increasing amount of TiN phase in the β-SiAlON matrix, and a similar trend was also observed by Lee et al., [31].

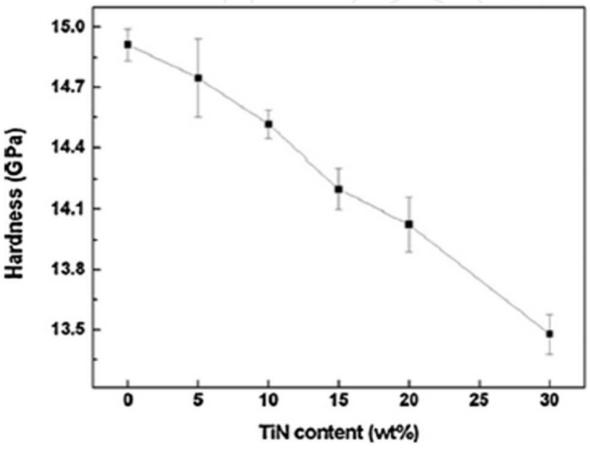

Figure 8. Vickers hardness of TiN/Si_3N_4 composites with various TiN content.

http://dx.doi.org/10.5772/50547

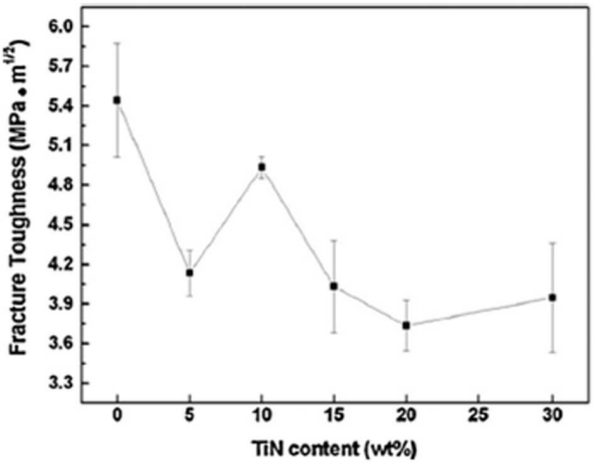

Figure 9. Fracture toughness of TiN/Si_3N_4 composites measured by Vickers surface indentation technique for various TiN content.

Fracture toughness describes the ability of a material containing a crack to resist fracture, and is one of the most important properties of any material for virtually all design applications. It is also a quantitative way of expressing a material's resistance to brittle fracture when a crack is present. The fracture toughness of the composites containing various compositions of TiN measured by the indentation technique for composites is shown in Fig. 9. The monolithic Si_3N_4 ceramics have the highest value of 5.4 MPa.$m^{1/2}$.Among the TiN/Si_3N_4 composites, the toughness reaches a maximum value of 4.9 MPa.$m^{1/2}$ for the composite containing 10 wt% TiN, whereas the other composites have values lower than 4.2 MPa.$m^{1/2}$. An equation derived by Buljan et al., 1988, which expresses the increase in toughness as function of grain size under the assumption that the grain shapes are the same, is given by

$$d K_c = C K_c^0 \left(\frac{dD}{D_0} - 1 \right) \tag{1}$$

Where C is a coefficient dependent on the mode of fracture; $K_c^{\ 0}$ and and D_0 are the initial toughness and grain size; dK_c and dD are the respective changes in toughness and diameter. Hence, the changes in grain size and shape are directly related to toughness. An increase in Si_3N_4 grain size results in increasing fracture toughness. Although the addition of TiN does not improve the mechanical properties of Si_3N_4 based composites, the special sintering behavior produced by pulse direct current (grain coarsening effect for Si_3N_4 based grain) may occur in a SPS process.

3. Conclusions

i. By utilizing Si_3N_4 and TiN nano powders as starting materials, a series of near-fully dense TiN/Si_3N_4 based nanocomposites containing varying TiN contents (5–30 wt %) have been fabricated successfully by a spark plasma sintering technique.

ii. A grain coalescence of the TiN phase has been demonstrated by TEM. The conductive TiN grains in the insulating Si_3N_4 matrix are observed to be isolated from each other. From the microstructural observations, the composites appear to be insulating materials.

iii. For the nanocomposite of 5 TN, 15 TN, 20 TN, and 30 TN, the TiN phase inhibits the grain growth of Si_3N_4 based grains during sintering. Hence, the nanosized Si_3N_4 based crystallites are maintained in size as the raw material.

iv. The spark plasma sintered TiN/Si_3N_4 based composite containing 10 wt% TiN achieves the largest grain size and the highest toughness of 4.9 MPa. $m^{1/2}$ compared to the other composites. A possible pulse current sintering mechanism might occur, which causes a temporary high temperature in the sintering compact, and then accelerates the grain coarsening of Si_3N_4 based grains.

Acknowledgements

Authors are thankful to National Science Council of Taiwan for its financial support under the contract No: NSC 99-2923-E-006-002-MY3 to carry out the present work.

Author details

Jow-Lay Huang* and Pramoda K. Nayak

*Address all correspondence to: JLH888@mail.ncku.edu.tw

National Cheng Kung University, Taiwan

References

[1] Ayas, E., Kara, A., & Kara, F. (2008, July). A novel approach for preparing electrically conductive α/β SiAlON-TiN composites by spark plasma sintering. *Journal of the Ceramic Society of Japan*, 116(1355), 2008, 812-814, 0914-5400.

[2] Buljan, S. T., Baldoni, J. G., & Huckabee, M. L. (1987). *Si_3N_4-SiC composite, American Ceramic Society Bulletin*, 66(2), 347-352, 0002-7812.

[3] Buljan, S. T., Baldoni, J. G., Neil, J., & Zilberstein, G. (1988). Dispersoid-toughened silicon nitride composites,. *ORNL/Sub/8522011/1, GTE*.

[4] Balakrishnan, S., Burnellgray, J. S., & Datta, P. K. (1995). in: S. Hampshire, M. Buggy, B. Meenan, N. Brown (eds.) Preliminary studies of TiN particulate-reinforced

Si(3)N(4) matrix composite (SYALON 501) following exposure in oxiding and oxychloridising environments. Key Engineering Matererials, 1013-9826 , 99(1), 279-290.

[5] Borsa, C. E., & Brook, R. J. (1995). Fabrication of Al_2O_3/SiC nanocomposites using a polymeric precursor for SiC. In Ceramic Transactions Ceramic. Processing and Science, The American Ceramic Society, H. Hausner, G. L. Messing and S.-I. Hirano, (Ed.), Westerville, OH , 51, 653-657.

[6] Borsa, C. E., Ferreira, H. S., & Kiminami, R. H. G. A. (1999, May). Liquid Phase Sintering of Al_2O_3/SiC Nanocomposites. *Journal of the European Ceramic Society*, 19(5), 1999, 615-621, 0955-2219.

[7] Blugan, G., Hadad, M., Janczak-Rusch, J., Kuebler, J., & Graule, T. (2005, April). Fractography, mechanical properties, and microstructure of commercial silicon nitride-titanium nitride composites. *Journal of the American Ceramic Society*, 88(4), 2005, 926-933, 1551-2916.

[8] Carroll, L., Sternitzke, M., & Derby, B. (1996, November). Silicon carbide particle size effects in alumina based nanocomposites. *Acta Meterialia,*, 44(11), 1996, 4543-4552, 1359-6454.

[9] Dusza, J., Šajgalík, P., & Steen, M. (1999). Fracture Toughness of Silicon Nitride/Silicon Carbide Nanocomposite at 1350°C. *Journal of the American Ceramic Society*, 82(12), 3613-3615, 1551-2916.

[10] Dusza, J., Kovalčík, J., Hvizdoš, P., Šajgalík, P., Hnatko, M., & Reece, M. (2004). Creep Behavior of a Carbon-Derived Si_3N_4-SiC Nanocomposite. *Journal of the European Ceramic Society*, 24(12), 3307-3315, 0955-2219.

[11] Deepa, K. S., Kumari, Nisha. S., Parameswaran, P., Sebastian, M. T., & James, J. (2009). Effect of conductivity of filler on the percolation threshold of composites. Applied Physics Letters, 0003-6951 , 94(14), 142902.

[12] Evans, A. G., & Charles, E. A. (1976, July). Fracture Toughness Determinations by Indentation. *Journal of the American Ceramic Society*, 59(7-8), 1976, 371-372, 1551-2916.

[13] Greil, P., Petzow, G., & Tanaka, H. (1987). Sintering and hipping of silicon nitride-silicon carbide composite materials, Ceramics International (September 1986) 0272-8842 , 13(1), 19-25.

[14] Gogotsi, Y. G. (1994). Review: particulate silicon nitride based composite. Journal of Materials Science, January (1994). 1573-4803 , 29(10), 2541-2556.

[15] Gao, L., Li, J. G., Kusunose, T., & Niihara, K. (2004, February). Preparation and properties of TiN-Si_3N_4 composites,. *Journal of the European Ceramic Society*, 24(2), 2004, 381-386, 0955-2219.

[16] Galusek, D., Sedláček, J., Švančárek, P., Riedel, R., Satet, R., & Hoffmann, M. (2007). The influence of post-sintering HIP on the microstructure, hardness, and indentation

fracture toughness of polymer-derived Al_2O_3-SiC nanocomposites. *Journal of the European Ceramic Society*, 27(2-3), 1237-1245, 0955-2219.

[17] Guo, Z., Blugan, G., Kirchner, R., Reece, M., Graule, T., & Kuebler, J. (2007, September). Microstructure and electrical properties of Si_3N_4-TiN composites sintered by hot pressing and spark plasma sintering,. *Ceramics International*, 33(7), 2007, 1223-1229, 0272-8842.

[18] Herrmann, M., Balzer, B., Schubert, C., & Hermel, W. (1993). Densification, microstructure and properties of Si_3N_4-Ti(C,N) composites. *Journal of the European Ceramic Society*, 12(4), 287-296, 0955-2219.

[19] Huang, J. L., Chen, S. Y., & Lee, M. T. (1994). Microstructure, chemical aspects and mechanical properties of TiB_2/Si_3N_4 and TiN/Si_3N_4 composites. Journal of Materials Research, 0884-2914 , 9(9), 2349-2354.

[20] Huang, J. L., Lee, M. T., Lu, H. H., & Lii, D. F. (1996). Microstructure, fracture behavior and mechanical properties of TiN/Si3N4 composites, *Materials Chemistry and Physics*, 45(3), 203-210, 0254-0584.

[21] Kawano, S., Takahashi, J., & Shimada, S. (2002). Highly electroconductive TiN/Si_3N_4 composite ceramics fabricated by spark plasma sintering of Si_3N_4 particles with a nano-sized TiN coating. *Journal of Materials Chemistry*, 12(2), 361-365, 1364-5501.

[22] Kawano, S., Takahashi, J., & Shimada, S. (2003, April). Fabrication of TiN/Si_3N_4 ceramics by spark plasma sintering of Si_3N_4 particles coated with nanosized TiN prepared by controlled hydrolysis of $Ti(O\text{-}i\text{-}C_3H_7)_4$. *Journal of the American Ceramic Society*, 86(4), 2003, 701-705, 1551-2916.

[23] Kašiarová, M., Dusza, J., Hnatko, M., Lenčéš, Z., & Šajgalík, P. (2002). Mechanical Properties of Recently Developed Si3N4 + SiC Nanocomposites. *Key Engineering Materials*, 223, 233-236, 1013-9826.

[24] Kašiarová, M., Rudnayová, E., Kovalčík, J., Dusza, J., Hnatko, M., Šajgalík, P., & Merstallinger, A. (2003). Wear and creep characteristics of a carbon-derived Si_3N_4/SiC micro/nanocomposite. Materialwissenschaft und Werkstofftechnik, April (2003). 1521-4052 , 34(4), 338-342.

[25] Kašiarová, M., Dusza, Ján., Hnatko, M., Šajgalík, P., & Reece, M. J. (2006). Fractographic Montage for a Si_3N_4-SiC Nanocomposite. Journal of the American Ceramic Society May (2006). , 1551-2916 , 89(5), 1752-1755.

[26] Lee, B. T., Yoon, Y. J., & Lee, K. H. (2001, January). Microstructural characterization of electroconductive Si3N4-TiN composites,. *Materials Letters*, 47(1-2), 2001, 71-76, 0016-7577X.

[27] Lide, D. R. (2002). Experimental Data: Evaluation and Quality Control. CRC Handbook of Chemistry and Physics 83rd ed. CRC Press Boca Raton April (2002).

[28] Liu, C. C., & Huang, J. L. (2003). Effect of the electrical discharge machining on strength and reliability of TiN/Si_3N_4 composites. *Ceramics International*, 29(6), 679-687, 0272-8842.

[29] Liu, X. K., Zhu, D. M., & Hou, W. C. (2006). Microwave permittivity of SiC-$A1_2O_3$ composite powder prepared by sol-gel and carbothermal reduction. *Transactions of Nonferrous Metals Society of China*, 16, s494-s497, 1003-6326.

[30] Liu, J., Shen, Z. J., Nygren, M., Kan, Y. M., & Wang, P. L. (2006). SPS processing of bismuth-layer structured ferroelectric ceramics yielding highly textured microstructures. *Journal of the European Ceramic Society*, 26(15), 3233-3239, 0955-2219.

[31] Lee, C. H., Lu, H. H., Wang, C. A., Nayak, P. K., & Huang, J. L. (2011, March). Influence of Conductive Nano-TiC on Microstructural Evolution of Si3N4-Based Nanocomposites in Spark Plasma Sintering. *Journal of the American Ceramic Society*, 94(3), 2011, 959-967, 1551-2916.

[32] Martin, C., Mathieu, P., & Cales, B. (1989). Electrical discharge machinable ceramic composite. *Materials Science and Engineering: A*, 109, 351-356, 0921-5093.

[33] Niihara, K., & Hirai, T. (1986). Super-Fine Microstructure and Toughness of Ceramics. *Bull. Cerum. Soc. Jpn.*, 21(7), 598-604.

[34] Niihara, K., & Nakahira, A. (1988). Strengthening of oxide ceramics by SiC and Si_3N4 dispersions. In: Proceedings of the Third International Symposium on Ceramic Materials and Components for Engines, The American Ceramic Society, V. J. Tennery, (Ed.), Westerville, Ohio , 919-926.

[35] Niihara, K., & Nakahira, A. (1991). Strengthening and toughening mechanisms in nanocomposite ceramics. *Ann. Chim. (Paris)*, 16, 479-486, 0151-9107.

[36] Niihara, K. (1991). New design concept for structural ceramics-Ceamic nanocomposites. *The Centennial Memorial Issue of The Ceramic Society of Japan*, 99(10), 974-982, 0914-5400.

[37] Nakahira, A., Sekino, T., Suzuki, Y., & Niihara, K. (1993). High-temperature creep and deformation behavior of Al_2O_3/SiC nanocomposites. *Ann. Chim. (Paris)*,, 18, 403-408, 0151-9107.

[38] Ohji, T., Nakahira, A., Hirano, T., & Niihara, K. (1994). Tensile creep behavior of Alumina/ Silicon carbide nanocomposite. *Journal of the American Ceramic Society*, 77(12), 3259-3262, 1551-2916.

[39] Ohji, T., Jeong-K, Y., Choa-H, Y., & Niihara, K. (1998, June). Strengthening and toughening mechanisms of ceramic nanocomposites. *Journal of the American Ceramic Society*, 81(6), 1998, 1453-1460, 1551-2916.

[40] Raichenko, A. I. (1985, January). Theory of metal powder sintering by an electric-pulse discharge. *Soviet Powder Metallurgy and Metal Ceramics*, 24(1), 1985, 26-30, 0038-5735.

[41] Ragulya, A. V. (2010). Fundamentals of Spark Plasma Sintering. Encyclopedia of Materials: Science and Technology , 978-0-08043-152-9 , 1-5.

[42] Smith, R. L., & Sandland, G. E. (1922). An Accurate Method of Determining the Hardness of Metals, with Particular Reference to Those of a High Degree of Hardness. Proceedings of the Institution of Mechanical Engineers , LCCN 0801 8925, I, 623-641.

[43] Sinha, S. N., & Tiegs, T. N. (1995). Fabrication and properties of Si_3N_4-TiN composite. Ceramic Engineering and Science Proceedings July (1995). , 0196-6219 , 16(4), 489-496.

[44] Šajgalík, P., Dusza, J., & Hoffmann, M. J. (1995). Relationship Between Microstructure, Toughening Mechanisms and Fracture Toughness of Reinforced β-Si_3N_4 Ceramics. *Journal of the American Ceramic Society,*, 78(10), 2619-2624, 1551-2916.

[45] Shen, Z., & Nygren, M. (2001). Kinetic aspects of superfast consolidation of silicon nitride based ceramics by spark plasma sintering,. *Journal of Materials Chemistry*, 11(1), 204-207, 0959-9428.

[46] Shen, Z. J., Peng, H., Liu, J., & Nygren, M. (2004). Conversion from nano- to micron-sized structures: Experimental observations. *Journal of the European Ceramic Society*, 24(12), 3447-3452, 0955-2219.

[47] Šajgalík, P., Hnatko, M., Lojanová, Š., Lenčéš, Z., Pálková, H., & Dusza, J. (2006). Microstructure, hardness, and fracture toughness evolution of hot-pressed SiC/Si_3N_4 nano/micro composite after high-temperature treatment. International Journal of Materials Research , 1862-5282 , 97(6), 772-777.

[48] Vollath, D., Szabó, D. V., & HauBelt, J. (1997). Synthesis and Properties of Ceramic Nanoparticles and Nanocomposites. *Journal of the European Ceramic Society,*, 17(11), 1317-1324, 0955-2219.

[49] Vollath, D., & Szabó, D. V. (2006). Microwave Plasma Synthesis of Ceramic Powders. In: Advances in Microwave and Radio Frequency Processing Part-IX, Springer , 619-626.

[50] Xu, Y., Nakahira, A., & Niihara, K. (1994). Characteristics of Al_2O_3-SiC nanocomposite prepared by sol-gel processing. *Journal of the Ceramic Society of Japan*, 102(3), 312-315, 0914-5400.

[51] Yoshimura, M., Komura, O., & Yamakawa, A. (2001, May). Microstructure and tribological properties of nano-sized Si 3N4. *Scripta Materialia*, 44(8-9), 2001, 1517-1521, 1359-6462.

[52] Zivkovic, L., Nikolic, Z., Boskovic, S., & Miljkovic, M. (2004, June). Microstructural characterization and computer simulation of conductivity in Si3N4-TiN composites,. *Journal of Alloys and Compounds*, 373(1-2), 2004, 231-236, 0925-8388.